

Role for CCR5 in Dissemination of Vaccinia Virus In Vivo[∇]

Ramtin Rahbar, Thomas T. Murooka, and Eleanor N. Fish*

Toronto General Research Institute, University Health Network, Toronto, Ontario M5G 2M1, Canada, and Department of Immunology, University of Toronto, Toronto, Ontario M5S 1A8, Canada

Received 4 August 2008/Accepted 4 December 2008

In an earlier report, we provided evidence that expression of CCR5 by primary human T cells renders them permissive for vaccinia virus (VACV) replication. This may represent a mechanism for dissemination throughout the lymphatic system. To test this hypothesis, wild-type CCR5^{+/+} and CCR5 null mice were challenged with VACV by intranasal inoculation. In time course studies using different infective doses of VACV, we identified viral replication in the lungs of both CCR5^{+/+} and CCR5^{-/-} mice, yet there were diminished viral loads in the spleens and brains of CCR5^{-/-} mice compared with CCR5^{+/+} mice. Moreover, in association with VACV infection, we provide evidence for CD4⁺ and CD8⁺ T-cell as well as CD11c⁺ and F4/80⁺ cell infiltration into the lungs of CCR5^{+/+} but not CCR5^{-/-} mice, and we show that the CCR5-expressing T cells harbor virus. We demonstrate that this CCR5 dependence is VACV specific, since CCR5^{-/-} mice are as susceptible to intranasal influenza virus (A/WSN/33) infection as CCR5^{+/+} mice. In a final series of experiments, we provide evidence that adoptive transfer of CCR5^{+/+} bone marrow leukocytes into CCR5^{-/-} mice restores VACV permissiveness, with evidence of lung and spleen infection. Taken together, our data suggest a novel role for CCR5 in VACV dissemination in vivo.

Vaccinia virus (VACV) is the best known member of the *Orthopoxvirus* genus of the *Poxviridae* and was used for the vaccine strain that led to the global eradication of smallpox (15). VACV has a large, double-stranded DNA genome of approximately 200 kb, a cytoplasmic site of replication, many virus-encoded enzymes for transcription and DNA replication, and a complex morphogenic pathway that produces distinct forms of infectious virions from each infected cell (36). Variola virus, the causative agent of smallpox, killed more people than any other pathogen in the history of mankind (12). In 1980, the World Health Organization (WHO) certified that the world was free of smallpox, but the potential for variola virus to be used as a potential biological weapon has led to renewed interest in the pathogenesis of smallpox and the development of therapies (6). While variola virus has a narrow natural host range in humans, with nonhuman primates exhibiting susceptibility in a laboratory setting (7), and while VACV exhibits a broader range of infectible hosts, both intranasal infections result in similar dissemination of virus: replication occurs initially in lymph nodes draining the upper respiratory tract, after which a transient viremia spreads virus to reticuloendothelial cells throughout the host. Notably, in variola alone, a second round of replication within these sites precedes a more intense secondary viremia and the subsequent clinical manifestations of the disease. Based on the pathogenic similarities, VACV presents a suitable model for variola virus infection (5, 19–22, 40).

Many poxviruses, including VACV, employ strategies to modulate chemokine activity, including virus-encoded chemokine-binding proteins (C23L/B29R encoded by VACV, G3R

encoded by variola virus, and DIL/H5R proteins encoded by cowpox virus) (1, 17, 31, 44) and receptor homologues (the K2R homologue of a CXCR encoded by swinepox virus and the Q2/3L homologue of a CCR encoded by caripoxvirus) (8, 29, 34, 37, 43). The involvement of chemokine receptors in poxviral infection was suggested in studies utilizing the rabbit poxvirus, myxoma virus. Specifically, CCR5 was implicated in mediating cell target susceptibility to infection in BGMK cells (30), which was later shown to correlate with intracellular signaling (27, 35). In a recent publication we provided evidence that virus activation of CCR5 leads to the selective activation of distinct signaling pathways that are advantageous for the virus (39). We demonstrated that VACV infection in permissive cells is inhibited by small interfering RNA knockdown of cell surface CCR5 expression and by the CCR5 antagonist TAK-779. The importance of tyrosine phosphorylation of CCR5 was suggested by the observation that introduction of a CCR5 mutant in which all the intracellular tyrosines are replaced by phenylalanines effectively reduces VACV infection in permissive cells. Moreover, tyrosine 339 was implicated in CCR5 as the critical residue for mediating viral infection, since cells expressing CCR5.Y339F do not support viral replication. The cascade of events that leads to the permissive phenotype of these cells includes phosphorylation activation of multiple signaling effectors, i.e., Jak-2, IRS-2, ERK1/2, and Grb2. These data were supported by findings that viral replication in permissive CCR5-expressing cells is blocked by herbimycin A and the Jak2 inhibitor tyroprostin AG490 but not by pertussis toxin. Viewed altogether, a critical role of postentry events, specifically intracellular tyrosine phosphorylation events, in determining permissiveness of cells to VACV replication was established. Furthermore, evidence was provided that introduction of CCR5 in primary human T cells renders them permissive to VACV replication. Since permissive infection of T cells might represent a mechanism for VACV dissemination throughout the lymphatic system, we hypothesize that the ab-

* Corresponding author. Mailing address: Toronto General Research Institute, 67 College Street, Rm. 424, Toronto, Ontario M5G 2M1, Canada. Phone: (416) 340-5380. Fax: (416) 340-3453. E-mail: en.fish@utoronto.ca.

[∇] Published ahead of print on 10 December 2008.

sence of CCR5 may be protective against VACV infection in vivo.

Several mouse models of VACV infection that differ in mouse and viral strains, as well as routes of virus inoculation, have provided insights into the immunopathogenesis of VACV in vivo (4, 26, 41). Here, employing an intranasal inoculation route of VACV infection, we provide supportive evidence for a role for CCR5 in VACV dissemination in vivo.

MATERIALS AND METHODS

Animals. CCR5^{-/-} mice (B6;129P2-Ccr5tm1Kuz) and mice from their genetically matched mouse strain were purchased from the Jackson Laboratory and housed in microisolator cages in the animal colony at the Canadian Blood Services Building and the Ontario Cancer Institute, the University Health Network. All experiments were performed using female mice, 6 to 8 weeks of age. Mouse studies were performed in an animal biosafety level 2 facility under a protocol approved by the University Health Network Animal Care Committee.

Viruses. VACV strain Western Reserve (WR) was a gift from Grant McFadden (University of Florida). A4L-enhanced green fluorescent protein (EGFP)-VACV (EGFP-VACV) was a gift from Geoffrey Smith (Imperial College of London) (9). Infection with either VACV WR or EGFP-VACV results in comparable infection and immune cell trafficking into bronchial alveolar lavage fluid (BAL), mediastinal lymph nodes (mLNs), and spleens of infected mice (data not shown). VACV was purified as described previously (39). Briefly, virus was grown in HeLa cells and purified by sedimentation through a 36% sucrose cushion, and the number of virus particles was determined by optical density measurement at 260 nm ($1 \text{ U} = 1.2 \times 10^{10}$ particles). The particle/PFU ratios of VACV (WR) and EGFP-VACV were estimated to be 40:1 and 50:1, respectively.

Virus infection. All viral infection studies were performed in a biosafety level 2 room. Mice were anesthetized by intraperitoneal injection with 50 μ l of ketamine (50 mg/kg)-xylazine (2.5 mg/kg) diluted in phosphate-buffered saline (PBS). Immediately, mice received an intranasal inoculation of 10^4 PFU of either VACV WR or EGFP-VACV suspended in 20 μ l of sterile PBS. Control mice received only sterile PBS (mock infection). VACV (or PBS alone) was instilled into the nares, and mice were observed until the virus was inhaled. Mice were monitored daily for any symptoms of disease and were weighed daily during the course of the experiment.

Tissue isolation and viral titration. Mice were sacrificed on days 0, 1, 3, and 7 postinfection (p.i.), at which times lungs, brains, mLNs, and spleens were removed and BAL fluid extracted for the indicated histology, viral titer, and molecular analyses. Samples for histology were either paraformaldehyde fixed and embedded in paraffin, or embedded in HistoPrep (Fisher Scientific), submerged in ice-cold isopentane, and then snap frozen in liquid nitrogen. Tissues for determination of viral titers were processed to generate cell suspensions, and then the cells were lysed by three successive freeze-thaw cycles. BAL fluid cells were likewise subjected to three successive freeze-thaw cycles. Virus titers were determined by plaque-forming assays on BS-C-1 cells. Specifically, 250 μ l of each of the lysed cell suspensions and 10-fold serial dilutions of each were transferred directly onto BS-C-1 monolayers in multiwell tissue culture dishes, incubated for 48 h, fixed, and stained with crystal violet, and then plaques were counted. Titers were calculated as PFU/g tissue and PFU/mouse for BAL fluid. The lower limit of detection is 120 plaques/g tissue and 180 plaques/mouse for BAL fluid.

Leukocyte isolation and flow cytometry. BAL fluid was collected from mock- and VACV-infected mice at the indicated time points p.i., as described previously (42). Briefly, CCR5^{+/+} and CCR5^{-/-} mice were sacrificed, and the lungs were flushed with 3 ml of PBS containing 10 U/ml heparin through a blunted 23-gauge needle inserted into the trachea. Erythrocytes in the pellets were lysed with 5 ml of ACK buffer (0.829% NH₄Cl, 0.1% KHCO₃, and 0.0372% Na₂EDTA, pH 7.4) for 5 min, followed by two washes with PBS. The spleen and mLNs from each mouse were excised and digested for 30 min in digestion buffer (5% calf serum, 1 mg/ml of collagenase [Roche Diagnostics] and 30 μ g/ml of DNase [Roche Diagnostics] in PBS). The digested tissue fragments were further dispersed by mashing and passing through a 0.7- μ m cell strainer. Erythrocytes in the pellets were lysed with 5 ml of ACK buffer for 5 min, followed by two washes with PBS to obtain a single-cell suspension.

Cells were stained for 45 min on ice with appropriate combinations of phycoerythrin (PE)-, PE-Cy5-, or allophycocyanin (APC)-labeled antibodies to CCR5 (clone HM-CCR5; eBioscience), CD4 (clone GK1.5; eBioscience), CD8 (clone 53-6.7; eBioscience), CD3 (clone145-2C11; BD Pharmingen), CD11c (clone

HL3; BD Pharmingen), F4/80 (clone BM8; eBioscience), and CD45 (clone 30-F11; eBioscience). The relevant isotype antibody controls were obtained from eBioscience and BD Pharmingen. After three washes with PBS, cells were fixed with 2% paraformaldehyde in PBS, washed, and then analyzed by fluorescence-activated cell sorting (FACS) (FACSAria). VACV-infected cells were detected based on the EGFP expression from the tagged virus. Data were analyzed using FACSDiva software (BD Biosciences) and are presented as the absolute number of positive cells within the gated population.

Histology and immunohistochemistry. (i) **Sample preparation.** Tissues that were embedded in HistoPrep and snap frozen in liquid nitrogen were sectioned at -20°C and then processed for immunohistochemistry. Specifically, thin sections were thawed at room temperature for 3 min, followed by fixation in methanol-acetone (50:50) at -20°C for 15 min, and then washed with PBS before immunostaining. For paraffin sections, samples were fixed overnight at room temperature in 2% paraformaldehyde, dehydrated through a series of ethanol washes, and processed for paraffin sectioning.

(ii) **Histological observations.** Paraffin sections were rehydrated and stained with hematoxylin-eosin, followed by standard histological protocols. Images were acquired with a Zeiss Axioplan 2 imaging microscope (Carl Zeiss, Canada Ltd.) equipped with bright-field capabilities and a digital AxioCam camera (Carl Zeiss, Canada Ltd.). Axio Vision 2.05 was used as the image acquisition software, and captured images were processed with Adobe Photoshop version 7.0 (Adobe Systems, Inc.).

(iii) **Immunohistochemical analysis.** Nonspecific antibody binding was blocked by incubating thin sections in blocking buffer (bovine serum albumin [0.5%, wt/vol] plus fish gelatin [0.2%, vol/vol] in PBS) for 30 min at room temperature, followed by incubation in wash buffer (BSA [0.5%, wt/vol] plus fish gelatin [0.1% vol/vol] in PBS). PE- or PE-Cy5 conjugated primary antibodies were appropriately diluted in blocking buffer, and thin sections were incubated at room temperature for 1 h. Antibodies against the following proteins CCR5 (1:500), CD4 (1:250), and CD8 (1:250) were used. The relevant isotype antibodies were used as controls.

Sections were analyzed by confocal microscopy, as described previously (39).

Bone marrow transplantation. Bone marrow-derived cells from CCR5^{+/+} donor mice were obtained by flushing the cavities of freshly dissected femurs with PBS. The suspension was then centrifuged through Ficoll-Hypaque (Amersham Biosciences) for 30 min at room temperature at $1,200 \times g$. Hematopoietic leukocytes at the interphase were extracted and washed three times with PBS. Recipient CCR5^{-/-} and CCR5^{+/+} control mice were irradiated with a sublethal dose of 1,100 cGy by whole-body irradiation (137 Cs; Gammacell 40). Four hours later, mice received 10^6 wild-type (CCR5^{+/+})-derived hematopoietic leukocytes via tail vein injection. At 2 weeks after bone marrow transplantation, mice received an intranasal inoculation of 10^4 PFU of VACV suspended in 20 μ l of sterile PBS. Mice were sacrificed at predetermined time points, and BAL fluid, lungs, mLNs, and spleens were harvested for FACS analysis and VACV titration.

Administration of TAK-779, a CCR5 antagonist. A CCR5 antagonist, TAK-779 (*N,N*-dimethyl-*N*-[4-[[[2-(4-methylphenyl)-6,7-dihydro-5H-benzocyclohepten-8-yl]carbonyl]amino]benzyl]tetra-hydro-2H-pyran-4-aminium chloride; molecular weight, 531.13) was kindly provided by Donald Branch (University of Toronto). TAK-779 was dissolved in 5% mannitol solution, and mice were injected subcutaneously with 150 μ g TAK-779 in a volume of 100 μ l at 1 day prior to infection and daily p.i.

Statistical analysis. Statistically significant differences in measured outcomes (other than virus titer) between groups of mice were determined by Student's *t* test using Microsoft Excel MAC v.X software. *P* values of <0.05 were considered significant. For differential analysis of tissue virus titers, for each tissue type we first fit a two-way analysis of variance (ANOVA) to evaluate the significance of all the data points in one set compared to all the data points in the comparator set (with two levels, CCR5^{+/+} versus CCR5^{-/-}). We then performed a Tukey honest significance difference test to compare the means of the levels of each data point conditional on the time point, using the ANOVA results.

RESULTS

CCR5^{-/-} mice are less susceptible to systemic VACV infection. To investigate the contribution of CCR5 to the pathogenesis of VACV infection, CCR5^{-/-} and CCR5^{+/+} mice were either mock infected or infected with 10^4 , 10^5 , or 10^6 PFU of VACV strain WR by intranasal inoculation and monitored daily for weight loss. Infection with 10^4 PFU of VACV resulted in approximately 8% weight loss in CCR5^{+/+} but

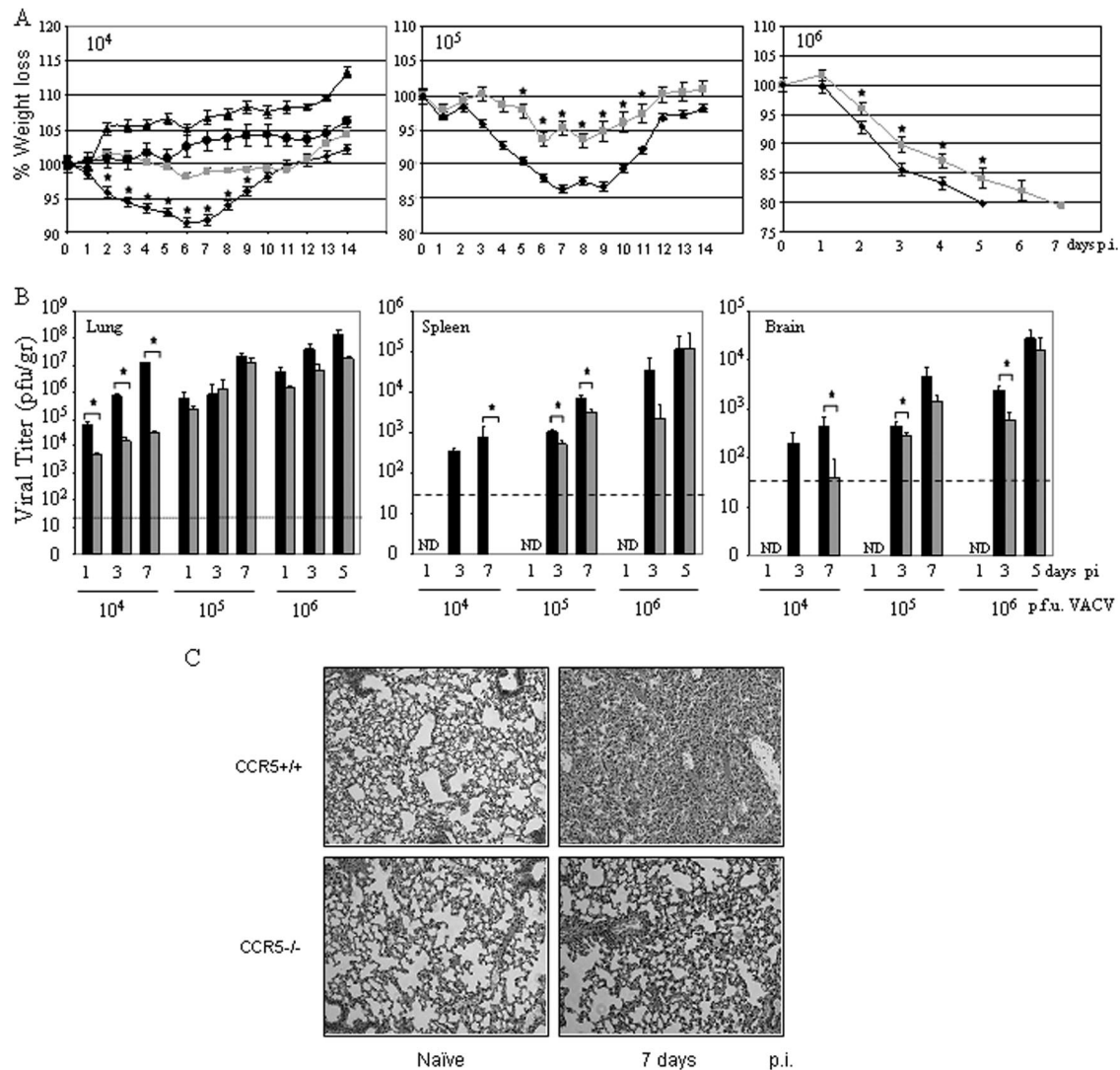


FIG. 1. CCR5^{-/-} mice are less susceptible to VACV infection. Groups of female mice age 6 to 8 weeks were either mock infected (PBS) or infected with 10⁴, 10⁵, or 10⁶ PFU of VACV by intranasal inoculation. (A) Body weight was measured daily, and values are recorded as the mean percent weight loss at the indicated time point compared to that of uninfected control mice ± standard error. 10⁴ PFU, *n* = 10; 10⁵ PFU, *n* = 12 until day 8 and *n* = 7 thereafter; 10⁶ PFU, *n* = 12 until day 3 and *n* = 7 thereafter. CCR5^{+/+} mock infected, ▲; CCR5^{+/+} VACV infected, ◆; CCR5^{-/-} mock infected, ●; CCR5^{-/-} VACV infected, ■. (B) Viral titers were measured in lungs, spleens, and brains of CCR5^{+/+} (■) and CCR5^{-/-} (□) mice (*n* = 10) at the indicated times p.i. with 10⁴ PFU of VACV, as described in Materials and Methods. (C) Lungs of mock-infected or VACV-infected (10⁴ PFU) CCR5^{+/+} and CCR5^{-/-} mice were harvested on day 7 p.i., fixed in 2% paraformaldehyde, and embedded in paraffin, and 6-μm-thick histological sections were prepared and stained with hematoxylin-eosin. The dotted line indicates the lower level of detection for VACV. *, *P* < 0.05. ND, not detected.

not CCR5^{-/-} mice (Fig. 1A), whereas mock infection had no effect on all mice. When infected with 10⁵ or 10⁶ PFU of VACV, both CCR5^{+/+} and CCR5^{-/-} mice exhibited weight loss, with a significantly greater weight loss in the CCR5^{+/+} mice (*P* < 0.05). When infected with 10⁵ PFU of VACV, CCR5^{+/+} mice exhibited approximately 14% weight loss, while CCR5^{-/-} lost approximately 7% of their body weight. At day 5 p.i., CCR5^{+/+} mice infected with 10⁶ PFU of VACV were euthanized, since they had lost 20% of their original body weight, while CCR5^{-/-} mice reached 20% weight loss at day 7 (Fig. 1A).

We next examined the lungs, spleens, and brain tissues of CCR5^{-/-} and CCR5^{+/+} mice for evidence of VACV. In ear-

lier studies, we provided evidence that VACV entry into cells is not mediated by CCR5, since virus enters both permissive and nonpermissive cells. A postentry event in T cells, mediated by CCR5, determines whether viral replication ensues (39). In the present study, examination of viral titers in the lungs of CCR5^{+/+} mice infected with 10⁴ PFU of VACV revealed a >3-fold log increase from 10⁴ to ~1.2 × 10⁷ PFU by day 7 p.i., in contrast to the lungs of the CCR5^{-/-} mice, where viral titers increased by <1 log, to 3.4 × 10⁴ PFU by day 7 p.i. (ANOVA indicates significant differences between all data points for CCR5^{+/+} and CCR5^{-/-} mice) (Fig. 1B). Comparable viral titers have been identified in the tracheae and lungs of mice after intranasal infection with VACV, with relatively low viral

loads in nasal washings (27). Accordingly, we focused our analyses on lung tissues. At 24 h p.i. we observe a log reduction in viral titer in the lungs of CCR5^{-/-} compared to the lungs of CCR5^{+/+} mice. Given our earlier data which suggested a role for CCR5 in viral permissivity (39) and the fact that T cells, resident monocytes, and macrophages, together with other potential target cells types (e.g., fibroblasts), express CCR5, this reduced pathogenesis in the CCR5^{-/-} mice was predicted. Notably, at the higher infective doses of 10⁵ and 10⁶ PFU of VACV, viral titers measured in the lung tissues of CCR5^{+/+} and CCR5^{-/-} mice on days 1, 3, 5, and 7 p.i. were comparable.

We next examined splenic viral titers as a measure of viral dissemination from the primary site of infection. At the infective dose of 10⁴ PFU of VACV, CCR5^{-/-} mice showed no evidence of virus in splenocytes (virus titers of <120 plaques/g tissue), in contrast to CCR5^{+/+} mice, where viral titers increased from day 1 to day 7 p.i. (>750 plaques/g tissue) (Fig. 1B) (ANOVA indicates significant differences at day 7 p.i. for splenic virus titers). At the higher infective dose of 10⁵ PFU of VACV, viral titers in the spleens of CCR5^{+/+} mice were significantly higher than viral titers in the spleens of CCR5^{-/-} mice. A similar trend was observed on day 3 p.i. in the spleens of mice inoculated with 10⁶ PFU of VACV, namely, higher viral titers in the CCR5^{+/+} compared with the CCR5^{-/-} mice.

We observed a similar trend in viral titers in the brains of CCR5^{+/+} and CCR5^{-/-} mice. Specifically, an intranasal inoculating dose of 10⁴ PFU of VACV resulted in measurable virus in the brains of CCR5^{+/+} on days 3 and 7 p.i., in contrast to the CCR5^{-/-} mice, where there was no detectable virus in their brains on day 3 p.i., with measurable, yet significantly lower viral titers on day 7 p.i. (Fig. 1B). At the higher infecting doses of VACV, virus was detected in the brains of CCR5^{+/+} and CCR5^{-/-} mice, although there were lower viral titers in the brains of the CCR5^{-/-} mice.

Viewed altogether, the data indicate that even when lung viral titers are comparable in CCR5^{+/+} and CCR5^{-/-} mice, viral dissemination to the spleens and brains of infected CCR5^{-/-} mice is reduced compared with viral dissemination in the infected CCR5^{+/+} mice.

VACV infection of CCR5^{+/+} but not CCR5^{-/-} mice leads to infiltration of CD4⁺ and CD8⁺ T cells into the lungs. At the infective dose of 10⁴ PFU of VACV, the lungs of CCR5^{+/+} mice exhibited inflammatory infiltrates and extensive histopathology by day 7 p.i., whereas no significant inflammatory cell influx or tissue destruction was observed in the lungs of CCR5^{-/-} mice (Fig. 1C). In addition, at this infective dose, CCR5^{+/+} mice exhibited a significant increase in the number of viable cells accumulating in the BAL fluid, in contrast to the case for the BAL fluid of CCR5^{-/-} mice: cell numbers in the BAL fluid from CCR5^{+/+} mice increased from 150,000 on day 0 to 320,000 by day 7 p.i., whereas cell counts in the BAL fluid of CCR5^{-/-} mice increased from 140,000 to 207,000 over the same time period (Fig. 2A). Moreover, in contrast to the increase in viral titers measured in the BAL fluid from CCR5^{+/+} mice from day 1 to day 7 p.i., we identified a negligible increase in viral titers in the BAL fluid from CCR5^{-/-} mice over the same time period (Fig. 2B).

To examine the inflammatory response that is associated with intranasal VACV infection at 10⁴ PFU, the composition of immune cells in the lungs of VACV-infected CCR5^{+/+} and

CCR5^{-/-} mice was characterized in time course studies. For this series of studies we employed EGFP-VACV. Notably, infection of CCR5^{+/+} mice with either 10⁴ PFU of VACV WR or 10⁴ PFU of EGFP-VACV results in comparable immune cell trafficking to BAL fluid, mLNs, and spleens (data not shown). Employing flow cytometry to identify inflammatory cell types, we provide evidence for CD4⁺ and CD8⁺ T-cell (CD3⁺) infiltration into the BAL fluid of CCR5^{+/+} but not CCR5^{-/-} mice during the course of VACV infection. Specifically, we observed a fivefold increase in CD4⁺ and an approximately eightfold increase in CD8⁺ T-cell influx in the BAL fluid by day 7 p.i. (Fig. 2C and E). The modest influx of CD4⁺ and CD8⁺ T cells into the BAL fluid of CCR5^{-/-} mice by day 1 p.i. was not sustained. Immunohistochemical staining of lung tissues from EGFP-VACV-infected CCR5^{+/+} and CCR5^{-/-} mice on day 7 p.i. for EGFP-VACV, CD4, and CD8 revealed a greater number of CD4⁺ and CD8⁺ T-cell infiltrates in the lungs of CCR5^{+/+} versus CCR5^{-/-} mice, with evidence of EGFP-VACV only in the CCR5-expressing CD4⁺ or CD8⁺ cells (data not shown). When flow cytometry was employed to quantitate the number of CCR5⁺ or CCR5⁻ CD4⁺ and CD8⁺ T cells that harbor EGFP-VACV in BAL fluid, the data revealed that the increase in CD4⁺ and CD8⁺ T-cell numbers in the BAL fluid of VACV-infected CCR5^{+/+} compared with VACV-infected CCR5^{-/-} mice is attributable to those CD4⁺ and CD8⁺ T cells that express CCR5 (Fig. 2D and F). At day 3 p.i. the increases in VACV-infected CD4⁺ T cells (Fig. 2D) and CD8⁺ T cells (Fig. 2F) were approximately fivefold and fourfold, respectively, in CCR5^{+/+} compared to CCR5^{-/-} mice. Interestingly, while total number of infected CD4⁺ and CD8⁺ T cells was approximately constant during the course of infection, the absolute numbers of CD4⁺ and CD8⁺ T cells increased in CCR5^{+/+} mice. One consideration is that a percentage of infected T cells may undergo apoptosis after infection. Certainly, VACV undergoes abortive replication in dendritic cells (DCs) (13) and induces apoptotic cell death in both DCs and macrophages. In addition, we propose that there is a constant egress of infected T cells from the lungs, for systemic spread of virus. When infected with 10⁵ PFU of VACV, both CCR5^{+/+} and CCR5^{-/-} mice exhibited infiltration of CD4⁺ and CD8⁺ T cells (CD3⁺) into the BAL fluid by day 7 p.i. Notably, the number of infiltrating T cells was significantly higher in the CCR5^{+/+} mice: 2.5 × 10⁵ versus 9 × 10⁴ for CD4⁺ and 2 × 10⁵ versus 6 × 10⁴ for CD8⁺ T cells (data not shown).

Expression of CCR5 influences the T-cell population of secondary lymphoid organs. Next, in time course studies during EGFP-VACV infection, we examined the CD4⁺ and CD8⁺ cell counts in the spleens and mLNs of CCR5^{+/+} and CCR5^{-/-} mice. Splenic CD4⁺ and CD8⁺ cell numbers decreased by day 3 p.i. for the CCR5^{+/+} mice yet remained unchanged in the CCR5^{-/-} mice (Fig. 3 A and B). By day 7 p.i. the numbers of splenic CD4⁺ and CD8⁺ cells rebounded to the original numbers in the CCR5^{+/+} mice.

In contrast to the trend observed in the spleens of infected CCR5^{+/+} mice, there was a significant increase in the numbers of CD4⁺ and CD8⁺ T cells in their mLNs by day 3 p.i., which further increased by day 7 p.i. (Fig. 3C and D). Specifically, for the CCR5^{+/+} mice, there was a ninefold increase in CD4⁺ and an eightfold increase in CD8⁺ T cells by day 7 p.i. CD4⁺ and

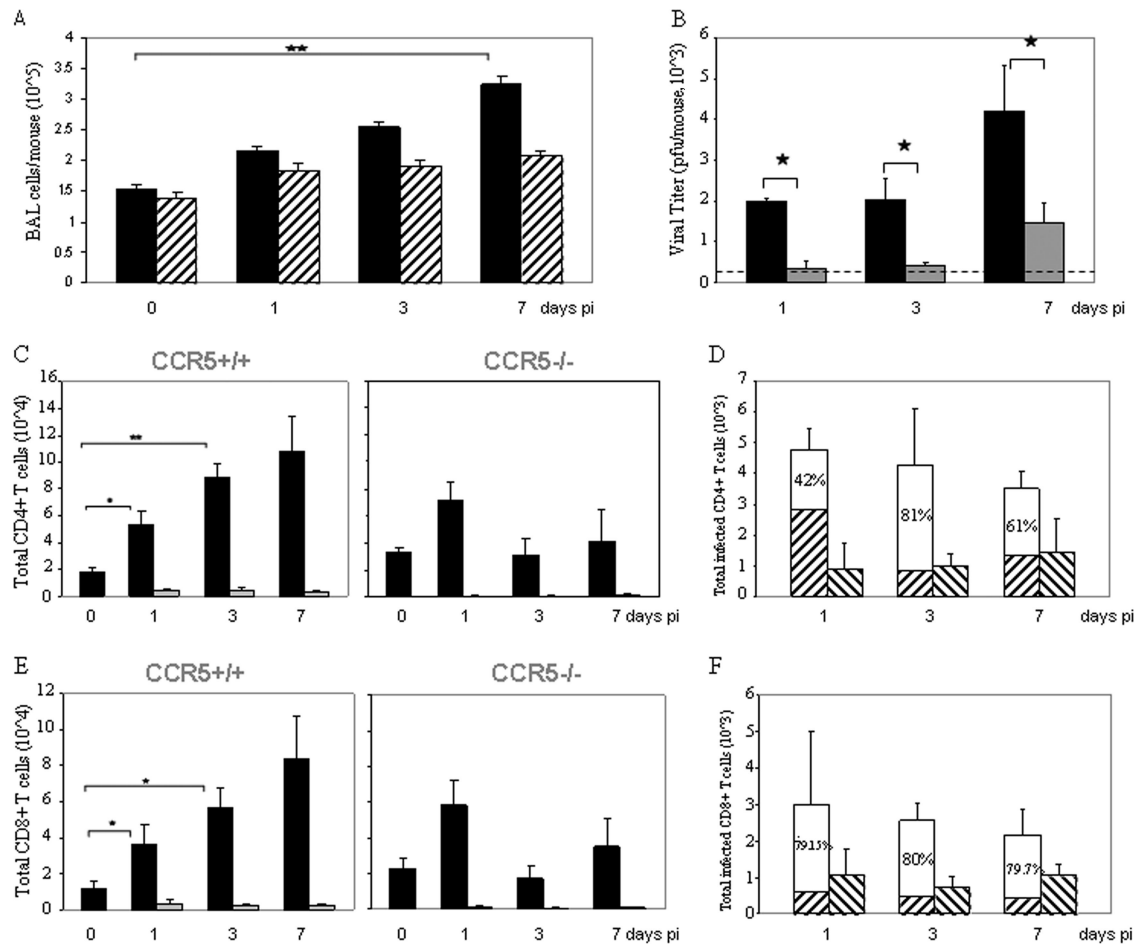


FIG. 2. Intranasal inoculation with VACV leads to an increase in BAL fluid viral titer and an influx of CD4⁺ and CD8⁺ T cells into the lungs of CCR5^{+/+} but not CCR5^{-/-} mice. Groups of female mice ($n = 10$), age 6 to 8 weeks, were infected with 10^4 PFU of EGFP-VACV by intranasal inoculation. Mice were euthanized at the indicated times p.i. and their BAL fluid collected as described in Materials and Methods. (A) Viable cell counts in the BAL fluid of CCR5^{+/+} (■) and CCR5^{-/-} (▨) were determined by trypan blue exclusion. Values are means \pm standard errors and are representative of two independent experiments. (B) Viral titers in BAL fluid of CCR5^{+/+} (■) and CCR5^{-/-} (▨) mice were measured at the indicated times p.i. The dotted line indicates the lower level of detection for VACV. (C and E) CD4⁺ (C) and CD8⁺ (E) T-cell counts were determined by flow cytometry, using PE-Cy5-conjugated anti CD4/CD8 and APC-conjugated CD3 antibodies. ■, total CD4⁺/CD8⁺ cell counts; ▨, VACV-infected CD4/CD8⁺ T cells as determined by quantitation of EGFP-positive cells as described in Materials and Methods. (D and F) The data are partitioned as VACV-infected CD4⁺ (D) and CD8⁺ (F) T cells in the BAL fluid of CCR5^{+/+} and CCR5^{-/-} mice, recorded as the percent positive \pm standard errors; results are representative of two independent experiments. ▨, CD4⁺ CCR5⁻/CD8⁺ CCR5⁻ T-cell count in the BAL fluid from CCR5^{+/+} mice; ▩, CD4⁺ CCR5⁻/CD8⁺ CCR5⁻ T-cell count in the BAL fluid from CCR5^{-/-} mice. *, $P < 0.05$; **, $P < 0.01$.

CD8⁺ T-cell numbers remained unchanged, at basal levels, in the mLNs of infected CCR5^{-/-} mice. As measured by staining for CD62 and CD69, the numbers of activated CD4⁺ and CD8⁺ T cells (CD62⁻ and CD69⁺) increased in the mLNs of CCR5^{+/+} but not CCR5^{-/-} mice by day 7 p.i., reflective of antigen stimulation. Specifically, in CCR5^{+/+} mice the number of CD4⁺ CD62⁻ T cells was approximately fivefold greater than the same population in CCR5^{-/-} mice (5×10^5 versus 1×10^5). Likewise, there was an approximately eightfold increase in CD4⁺ CD69⁺ T cells in the CCR5^{+/+} compared to the CCR5^{-/-} mice (1.6×10^5 versus 0.2×10^5), and an increased number of CD8⁺ CD62⁻ and CD8⁺ CD69⁺ T cells in the CCR5^{+/+} compared to the CCR5^{-/-} mice (2.2×10^5 versus 0.5×10^5 and 4.5×10^4 versus 0.7×10^4 , respectively) (data not shown). When infected with 10^5 PFU of VACV, both

CCR5^{+/+} and CCR5^{-/-} mice showed increased numbers of CD4⁺ and CD8⁺ T cells (CD3⁺) in their mLNs by day 7 p.i., with a significantly greater number in the CCR5^{+/+} mice: 6.3×10^5 versus 2.7×10^5 for CD4⁺ and 6×10^5 versus 3×10^5 for CD8⁺ T cells (data not shown).

TAK-779 reduces VACV dissemination. Data in a recent publication demonstrate that subcutaneous injection of TAK-779, a CCR5 antagonist, in a mouse model of asthma resulted in significantly diminished pulmonary inflammation. The analyses focused on BAL fluid and lung tissue (45). Expression of CCR5 in total lung cell suspensions was reduced in the TAK-779-treated mice compared to untreated mice. Additionally, the number of immune cells in affected lungs in mice treated with TAK-779 was also reduced. These findings are consistent with TAK-779 treatment disabling CCR5 signaling such that

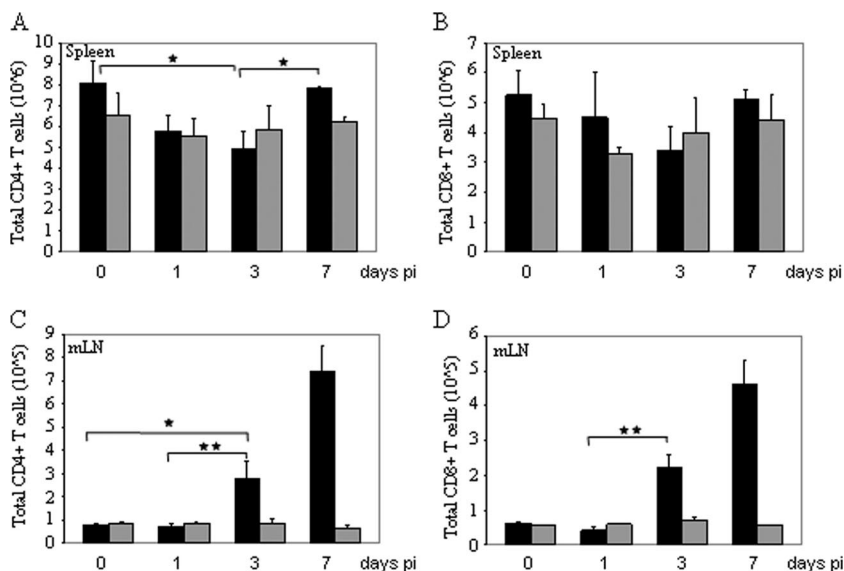


FIG. 3. VACV infection of CCR5^{+/+} but not CCR5^{-/-} mice influences the T-cell responses in secondary lymphoid organs. Groups of female mice ($n = 10$), age 6 to 8 weeks, were infected with 10^4 PFU of EGFP-VACV by intranasal inoculation. Mice were euthanized at the indicated times p.i., and CD3⁺ CD4⁺ and CD3⁺ CD8⁺ T-cell counts in the spleens (A and B) and mLN (C and D) were determined by flow cytometry, using PE-Cy5-conjugated anti CD4/CD8 and APC-conjugated CD3 antibodies. ■, total CCR5^{+/+} CD4⁺/CD8⁺; ▒, total CCR5^{-/-} CD4⁺/CD8⁺. Data are shown as mean cell counts \pm standard errors and are representative of two independent experiments. *, $P < 0.05$; **, $P < 0.01$.

chemokine-mediated cell trafficking is inhibited. Accordingly, to further examine the effects of CCR5 on VACV dissemination, CCR5^{+/+} mice were treated with 150 μ g of TAK-779 subcutaneously (49) 1 day prior to intranasal inoculation with VACV and thereafter daily for 7 days p.i. At day 7 p.i. mice were sacrificed, and their lungs and spleens were harvested and analyzed for evidence of virus infection. Notably, treatment with TAK-779 had no effect on lung viral titers but specifically reduced VACV dissemination to the spleens. Specifically, lung viral titers for both untreated and TAK-779 treated mice were 10^8 PFU/g tissue, whereas TAK-779 treatment resulted in reduced splenic virus titers from 1.2×10^3 PFU/g tissue in untreated mice to 4×10^2 PFU/g tissue in treated mice (data not shown).

Synchronous effects of VACV infection on antigen-presenting cells in CCR5^{+/+} and CCR5^{-/-} mice. Circulating naïve T cells encounter antigen in secondary lymphoid organs (spleens and LNs) presented by antigen-bearing CD11c⁺ DCs. In the context of a pulmonary influenza virus infection, DCs in the mLN present virus-specific antigen to naïve T cells, thereby invoking T-cell activation and proliferation and subsequent egress. The data in Fig. 4A demonstrate an increase in CD11c⁺ DCs by day 7 p.i. with VACV in the mLN of CCR5^{+/+} but not CCR5^{-/-} mice, consistent with the increase in T-cell numbers observed in the mLN of CCR5^{+/+} but not CCR5^{-/-} mice (Fig. 3C and D). By day 7 p.i., splenic DC numbers in the CCR5^{+/+} mice were elevated, yet they remained unchanged in the CCR5^{-/-} mice (Fig. 4B).

Similar to DCs, F4/80⁺ mature macrophages function as professional antigen-presenting cells. Accordingly, in time course studies we examined the influence of VACV infection on F4/80⁺ cell counts in the mLN and spleens of CCR5^{+/+} and CCR5^{-/-} mice. Consistent with the DC data, we provide evidence of an increase in F4/80⁺ cells by day 7 p.i. in the

mLN of CCR5^{+/+} but not CCR5^{-/-} mice (Fig. 4C). Additionally, by day 7 p.i. splenic F4/80⁺ cell counts in the CCR5^{+/+} mice were elevated, yet they remained unchanged in the CCR5^{-/-} mice (Fig. 4D). Viewing these findings together, we provide evidence that the higher viral loads in the lungs of CCR5^{+/+} mice result in increased mobilization of DCs and macrophages as antigen-presenting cells.

CCR5 expression does not contribute to influenza A/WSN/33 virus infection. To evaluate whether this CCR5 dependence for virus dissemination of a respiratory infection is VACV specific, CCR5^{+/+} and CCR5^{-/-} mice were infected with 0.1 hemagglutinin unit (HAU) of influenza A/WSN/33 virus via intranasal inoculation and monitored daily for symptoms of infection. As shown in Fig. 5A, in time course studies, infection with this dose of influenza A/WSN/33 virus resulted in approximately 5% weight loss in both CCR5^{+/+} and CCR5^{-/-} mice. We next examined sections of lung tissues from infected mice for evidence of cellular infiltrates. We observed an increase in cellular infiltrates into the lungs of both CCR5^{+/+} and CCR5^{-/-} mice by days 3 and 6 p.i. (Fig. 5B). In addition, comparable numbers of CD4⁺, CD8⁺, CD11c⁺, and F4/80⁺ cells were detected in the spleens and mLN of CCR5^{+/+} and CCR5^{-/-} infected mice on days 3 and 6 p.i. (data not shown).

We next examined the effects of higher inoculating doses of influenza A/WSN/33 virus in CCR5^{+/+} and CCR5^{-/-} mice. CCR5^{+/+} and CCR5^{-/-} mice were infected with 1 and 5 HAU of influenza A/WSN/33 virus via intranasal inoculation and monitored daily for symptoms of infection. In time course studies both CCR5^{+/+} and CCR5^{-/-} mice exhibited weight loss, with evidence of greater weight loss in CCR5^{-/-} mice. On days 9 and 10 p.i. with 1 HAU of virus, CCR5^{-/-} and CCR5^{+/+} mice were euthanized, respectively, since they had lost >20% of their original body weight. Similarly, all mice infected with 5 HAU were sacrificed on day 5 p.i. because of

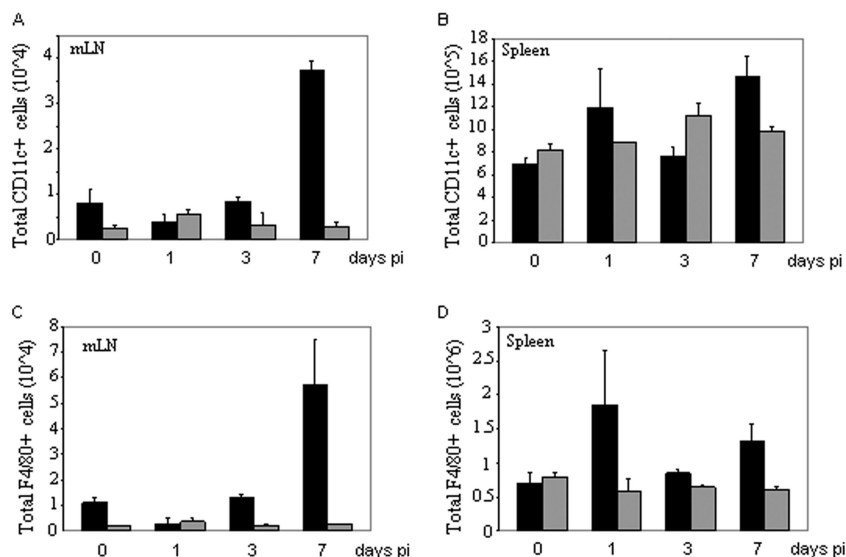


FIG. 4. VACV infection modulates CD11c⁺ DC and F4/80⁺ macrophage populations in the mLN and spleens of CCR5^{+/+} but not CCR5^{-/-} mice. CD11c⁺ and F4/80⁺ cell infiltration into the mLN (A and C) and spleens (B and D) of EGFP-VACV-infected mice (10⁴ PFU) was determined by flow cytometry, using APC-conjugated anti-CD11c and PE-Cy5-conjugated anti-F4/80 antibodies. Data are presented as total cell number infiltrate of CD11c⁺/F4/80 cells. ■, total CCR5^{+/+} CD11c⁺/F4/80⁺; □, total CCR5^{-/-} CD11c⁺/F4/80⁺. Data are shown as mean cell counts ± standard errors and are representative of two independent experiments. *, $P < 0.05$; **, $P < 0.01$.

weight loss. Examination of lung tissue thin sections for evidence of cellular infiltrates revealed extensive cellular infiltrates into the lungs of both CCR5^{+/+} and CCR5^{-/-} mice infected with 1 and 5 HAU of virus (data not shown). Flow cytometry analysis provided evidence for higher CD4⁺, CD8⁺, CD11c⁺, and F4/80⁺ cell numbers in the BAL fluid of CCR5^{-/-} mice compared to CCR5^{+/+} mice when infected with 5 HAU of virus, in agreement with previously reported data (29), and comparable infiltrating cell numbers by days 3 and 6 p.i. when mice were infected with 1 HAU of the virus (data not shown). Similar numbers of CD4⁺, CD8⁺, CD11c⁺, and F4/80⁺ cells were observed in the spleens and mLN of CCR5^{+/+} and CCR5^{-/-} infected mice after infection with either dose of influenza A/WSN/33 virus (data not shown).

Adoptive transfer of CCR5^{+/+} leukocytes into CCR5^{-/-} mice restores susceptibility to VACV infection. To confirm that CCR5 expression contributes to the pathogenesis of VACV infection *in vivo*, we adoptively transferred bone marrow-derived leukocytes from CCR5^{+/+} donor to both CCR5^{-/-} and CCR5^{+/+} recipient mice. CCR5^{+/+} and CCR5^{-/-} mice were irradiated with a sublethal dose of 1,100 cGy and, at 4 h postirradiation, received 10⁶ hematopoietic leukocytes from CCR5^{+/+} donor mice. At 2 weeks posttransplantation, all mice were infected with 10⁴ PFU of VACV by intranasal inoculation. Mice were sacrificed at the indicated times p.i., at which times BAL fluid was extracted and lungs, mLN, and spleens harvested.

Adoptive transfer of bone marrow-derived hematopoietic leukocytes from CCR5^{+/+} mice into CCR5^{-/-} mice partially restored susceptibility to VACV infectivity, as measured by viral titers in lung, BAL fluid, and spleens and corroborated by the extent of CD4⁺ and CD8⁺ cell infiltrates into the BAL fluid (Fig. 6). Specifically, the data in Fig. 6A indicate that there were similar trends of increasing viral titers in the lungs,

BAL fluid, and spleens of both CCR5^{+/+} and CCR5^{-/-} mice that received donor CCR5^{+/+} leukocytes, albeit lower overall titers in the CCR5^{-/-} recipients. Furthermore, by day 7 p.i. there was a fourfold increase in CD4⁺ and an eightfold increase in CD8⁺ T-cell infiltrates in the BAL fluid of CCR5^{-/-} leukocyte recipients, compared with fourfold and sixfold increases in CD4⁺ and CD8⁺ T-cell infiltrates in the BAL fluid of the CCR5^{+/+} recipients (Fig. 6B and C). Interestingly, when comparing the CCR5^{-/-} mice with CCR5^{-/-} mice that received donor CCR5^{+/+} leukocytes, the latter displayed a significant increase in the number of VACV-infected CD4⁺ and CD8⁺ cells. The majority of these infected cells were CCR5 positive. Unlike the CCR5^{-/-} mice, the CCR5^{-/-} mice that received donor CCR5^{+/+} leukocytes had CD4⁺ and CD8⁺ T cell numbers similar to those of the CCR5^{+/+} mice in their spleens (Fig. 6D and E) and mLN (Fig. 6F and G).

The number of CD11c⁺ cells increased significantly by day 3 p.i. in the BAL fluid (Fig. 6H), spleens (Fig. 6I), and mLN (Fig. 6J) of recipient CCR5^{+/+} mice, and similar trends were observed in the BAL fluid and mLN of recipient CCR5^{-/-} mice that received donor CCR5^{+/+} leukocytes. This increase in CD11c⁺ cells was not observed in the spleens of the CCR5^{-/-} mice that received donor CCR5^{+/+} leukocytes (Fig. 6I).

In other analyses, we examined F4/80⁺ cell counts in the BAL fluid, spleens, and mLN of CCR5^{+/+} and CCR5^{-/-} recipient mice at different times p.i. The results in Fig. 6 reveal that adoptive transfer of CCR5^{+/+} leukocytes into CCR5^{+/+} and CCR5^{-/-} mice resulted in similar levels of F4/80⁺ cells in their BAL fluid (Fig. 6K), spleens (Fig. 6L), and mLN (Fig. 6M).

Viewed together, the data strongly support a role for the donor CCR5^{+/+} leukocytes in mediating permissiveness to VACV infection and dissemination.

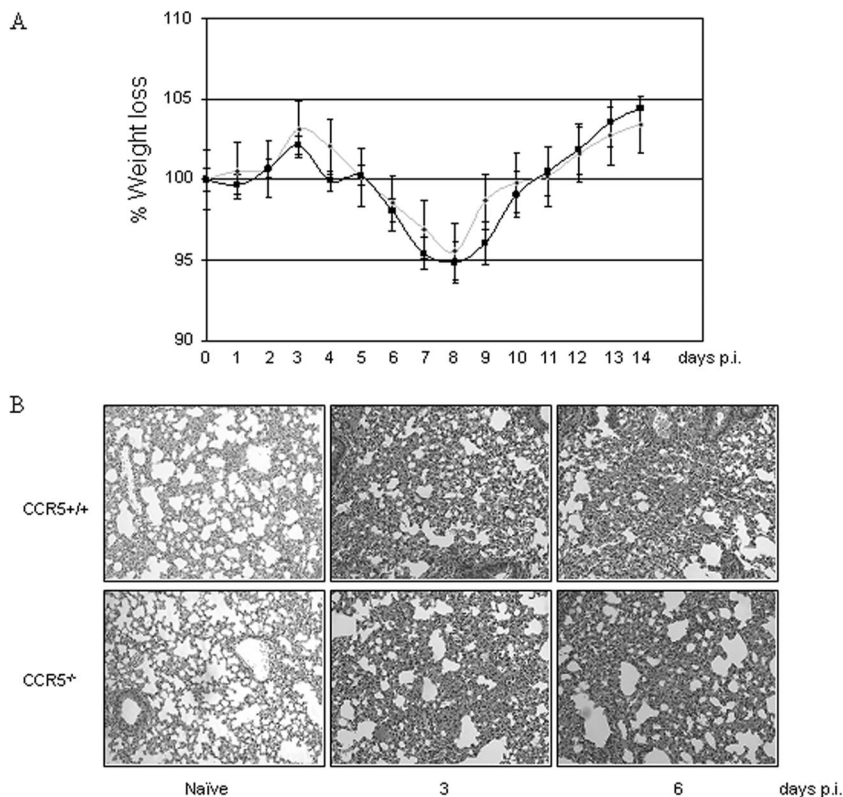


FIG. 5. CCR5^{-/-} mice are permissive for influenza A/WSN/33 virus infection. (A) Groups of female mice (*n* = 6), age 6 to 8 weeks, were infected with 0.1 HAU influenza A/WSN/33 virus and body weight measured daily. Body weight loss was expressed as the mean percent weight loss of animals at the indicated time points compared to that of controls ± standard errors. ■, CCR5^{+/+}; □, CCR5^{-/-}. (B) Lungs of mock- and influenza A/WSN/33 virus-infected CCR5^{+/+} and CCR5^{-/-} mice harvested on days 3 and 6 p.i. were fixed in 2% paraformaldehyde and embedded in paraffin, and 6-μm-thick histological sections were prepared and stained with hematoxylin and eosin.

DISCUSSION

In an effort to recapitulate the human disease, we have employed VACV as the surrogate for variola virus and the respiratory tract as the site of virus inoculation (14, 46, 48). The pathogenesis of VACV strain WR infection after intranasal inoculation is extensive respiratory infection followed by viremia leading to systemic infection, with considerable lethality at high doses of virus. The details of viral dissemination and pathogenesis are not well understood. The rapid systemic infection with WR is accompanied by dissemination of the virus to the brain and visceral tissue, including the spleen. Infection at nonlethal doses invokes immune cell infiltration to the lungs, and the virus is cleared by 15 days p.i.

Here we provide an analysis of the cellular immune response that accompanies intranasal VACV infection and demonstrate the importance of CCR5 expression for viral dissemination in a mouse model of the disease. VACV undergoes abortive replication in DCs (13) and induces apoptotic cell death in both DCs and macrophages (13, 24), whereas productive infection occurs in activated, but not resting, T cells (10). Indeed, following infection of mice with VACV, a robust T-cell response is elicited, associated with activated VACV-specific CD8⁺ T cells and CD4⁺ T cells (18, 41).

In activated T cells, susceptibility to infection is associated with the expression of a binding receptor that is induced de

novo upon T-cell activation (10, 16). When human peripheral blood T cells are activated with phytohemagglutinin and interleukin-12 (25), we observe the inducible de novo ectopic expression of CCR5 (data not shown). We speculate that inducible CCR5 expression upon T-cell activation may render cells permissive to VACV replication. It has been suggested that the productive infection of a subpopulation of activated T cells may account for dissemination of the virus away from local sites of inoculation (50), which is supported by our data here.

We provide several lines of evidence that suggest that trafficking of CD4⁺ and CD8⁺ T cells expressing CCR5 to the VACV-infected mouse lung is critical for subsequent dissemination of the virus. First, VACV-inoculated CCR5^{-/-} mice displayed markedly reduced accumulation of CD4⁺ and CD8⁺ T cells in their BAL fluid. Second, the majority of VACV infected CD4⁺ and CD8⁺ T lymphocytes in BAL fluid of CCR5^{+/+} were CCR5 positive. Third, at the lower infecting doses of VACV, there were reduced levels of virus in the spleens and brains of CCR5^{-/-} mice compared with CCR5^{+/+} mice. When bone marrow leukocytes from CCR5^{+/+} mice were adoptively transferred into CCR5^{-/-} mice, we observed a greater leukocyte accumulation in the BAL fluid of transplanted CCR5^{-/-} mice after VACV infection, and this coincided with viral dissemination to the spleen. Notably, although VACV-infected DCs and macrophages were identified in the

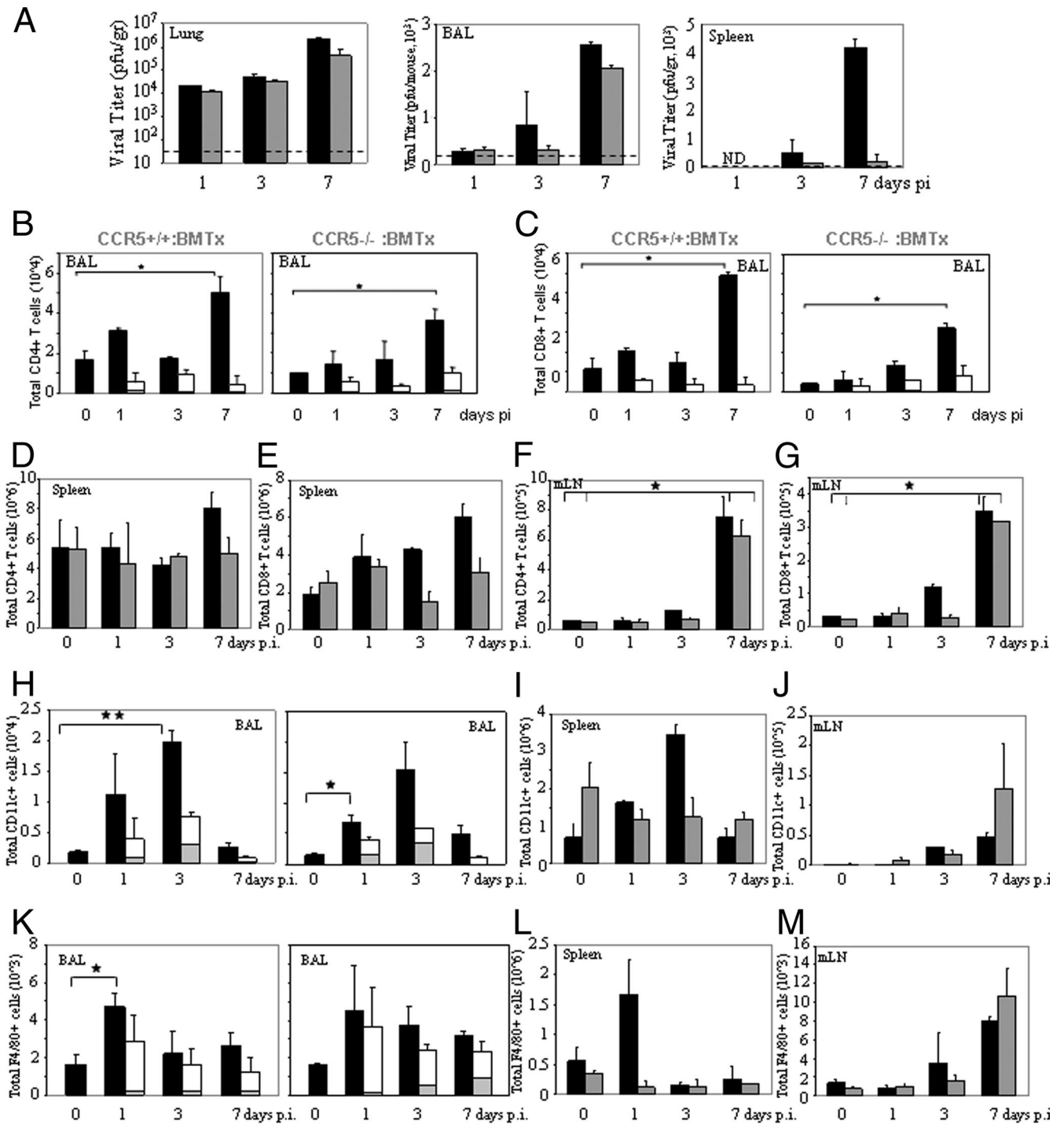


FIG. 6. Adoptive transfer of CCR5^{+/+} leukocytes into CCR5^{-/-} mice restores permissiveness to VACV infection. Hematopoietic leukocytes from CCR5^{+/+} mice were isolated and transplanted into irradiated CCR5^{+/+} and CCR5^{-/-} mice as described in Materials and Methods. After 2 weeks, transplanted mice were either mock or EGFP-VACV infected (10⁴ PFU). (A) At the indicated times p.i., mice were euthanized and VACV titers in lungs, BAL fluid, and spleens of recipient CCR5^{+/+} (■) and CCR5^{-/-} (□) mice were determined. The data are representative of two independent experiments. The dotted line indicates the lower level of detection for VACV. ND, not detected. (B to M) Single-cell suspensions from the BAL fluid, spleens, and mLNs of recipient CCR5^{+/+} (■) and CCR5^{-/-} (□) mice were obtained and stained with PE-Cy5-conjugated anti-CD4/CD8/F480 and APC-conjugated anti-CD3/CD11c antibodies at the indicated time points. Values are the mean CD4⁺ (B, D, and F) and CD8⁺ (C, E, and G) T-cell, CD11c⁺ cell (H, I, and J), and F4/80⁺ cell (K, L, and M) counts ± standard errors from two independent experiments. ■, total VACV-infected CCR5^{+/+} CD4⁺/CD8⁺ cells; □, total VACV-infected CCR5^{-/-} CD4⁺/CD8⁺/CD11c⁺/F4/80⁺ cells. *, *P* < 0.05; **, *P* < 0.01.

lungs of infected mice, examination of the mLN and spleens of mice p.i. showed no evidence of infected DCs or macrophages, from which we infer that these immune cells are not associated with harboring virus for viral dissemination. When infected with a higher dose of VACV, CCR5^{-/-} mice consistently exhibited a level of resistance to infection. When infected with 10⁵ PFU of VACV, CCR5^{+/+} mice lost approximately 14% of their body weight by day 7 p.i., whereas CCR5^{-/-} mice lost approximately 7% of their body weight. When infected with 10⁶ PFU of VACV, CCR5^{+/+} mice lost approximately 20% of their body weight by day 5 p.i., whereas CCR5^{-/-} mice reached 20% weight loss by day 7 p.i. Animal ethics guidelines require euthanization of mice at 20% loss of body weight; therefore, all mice were sacrificed when they reached this weight loss. Accordingly, we are unable to determine whether the absence of CCR5 influences lethality or mortality rates at this high inoculating dose of VACV. Nevertheless, a delay of 2 days in disease progression is notable given the overwhelming viral inoculating dose. In addition, viral titers in the spleens and brains of the CCR5^{-/-} mice were reduced by more than twofold when mice were infected with 10⁵ PFU. By day 3 p.i., viral titers in the spleens of the CCR5^{-/-} mice were reduced by more than a log fold, and those in the brains were reduced by approximately fourfold, compared to titers in the CCR5^{+/+} mice. At the higher infecting doses of VACV (10⁵ and 10⁶ PFU), lung viral titers were indistinguishable between CCR5^{+/+} and CCR5^{-/-} mice, yet VACV dissemination to the spleens and brains of CCR5^{-/-} mice was clearly reduced compared with that in CCR5^{+/+} mice, in support of a role for CCR5 in virus dissemination.

Administration of TAK-779, a CCR5 antagonist, reduced viral dissemination to the spleens of CCR5^{+/+} mice, with no effect on viral lung titers. TAK-779 inhibits the migration of leukocytes, including T cells, and abrogates CCR5-inducible signaling *in vivo* (45, 49). The dose of TAK-779 administered to the CCR5^{+/+} mice may have been insufficient to inhibit all expressed receptors (CCR5), which may have allowed for residual viral replication in the lung T cells. This would contrast with the CCR5^{-/-} mouse T cells, where no virus replication would occur. In addition, given that VACV infects cells of different lineages, including those that may not express CCR5, we might expect viral replication to be unaffected in some cell types. We speculate that a TAK-779-mediated reduction of CCR5-positive T-cell trafficking to the primary site of infection, the lungs, together with the TAK-779 inhibition of CCR5-mediated signaling in a percentage of these T cells, required for VACV replication (24), may be reflected in the subsequent reduction of VACV dissemination to the spleen. Taken together, these data further support our hypothesis that CCR5 is important for VACV dissemination *in vivo*.

The role of CCR5 in viral pathogenesis is virus specific. In a mouse model of West Nile virus infection, expression of CCR5 is crucial for viral clearance (16). Human immunodeficiency virus utilizes CCR5 as a coreceptor to mediate virus entry into target cells (32). In our studies, intranasal infection with influenza virus A/WSN/33 resulted in similar symptoms of disease in all mice, namely, weight loss and comparable influx of CD4⁺, CD8⁺, CD11c⁺, and F4/80⁺ cells in CCR5^{-/-} and CCR5^{+/+} mice, in the different tissue compartments examined. These results are consistent with earlier studies that have

reported that CCR5 does not play a role in influenza A virus pathogenesis (47). Infection of alveolar epithelial cells with the mouse-adapted influenza A virus strain PR/8 strongly induces the release of monocyte chemoattractants CCL2 and CCL5, followed by a strong monocyte transepithelial migration. This monocytic response is strictly dependent on CCR2, but not CCR5, expression (11, 23). In fact, when infected with influenza A virus, CCR5^{-/-} mice exhibited a hyperinflammatory response, expressed as increased pulmonary inflammation and higher mortality (11). In a murine model of colitis, CCR5-deficient mice showed increased infiltration of CD4⁺ and NK1.1⁺ lymphocytes, along with a decrease in Th1 and an increase in Th2 cytokine expression (2), providing additional evidence that the absence of CCR5 expression per se does not prevent immune cell trafficking to a site of infection or inflammation. Of note, none of these studies address the heightened immune response in the CCR5^{-/-} mice.

Our data clearly show that the adoptive transfer of bone marrow-derived CCR5^{+/+} leukocytes into CCR5^{-/-} mice partially rescued the permissive phenotype to VACV. Specifically, we observed increased infiltration of CD4⁺ and CD8⁺ T cells as well as CD11c⁺ and F4/80⁺ cells into the lungs, and increased VACV dissemination into the spleens, of transplanted CCR5^{-/-} mice.

Despite the reported redundancy associated with some chemokine-receptor interactions (3, 28, 33, 38, 47), here we provide evidence that CCR5 is important for the migration of T cells into affected lungs following intranasal VACV infection. Furthermore, the data demonstrate that CCR5 expression in T cells contributes to dissemination of VACV beyond the lung tissue. The data suggest that the role of CCR5 in VACV infection is not redundant, and we infer that CCR5 may be required for systemic VACV infection *in vivo*.

ACKNOWLEDGMENTS

This work was supported by grants from the Natural Sciences and Engineering Research Council of Canada to E.N.F. (NSERC 278397). R.R. and T.T.M. are recipients of CIHR doctoral research awards. E.N.F. is a Canada Research Chair.

We thank Carole Galligan for scientific discussions.

REFERENCES

- Alcami, A., J. A. Symons, P. D. Collins, T. J. Williams, and G. L. Smith. 1998. Blockade of chemokine activity by a soluble chemokine binding protein from vaccinia virus. *J. Immunol.* **160**:624–633.
- Andres, P. G., P. L. Beck, E. Mizoguchi, A. Mizoguchi, A. K. Bhan, T. Dawson, W. A. Kuziel, N. Maeda, R. P. MacDermott, D. K. Podolsky, and H. C. Reinecker. 2000. Mice with a selective deletion of the CC chemokine receptors 5 or 2 are protected from dextran sodium sulfate-mediated colitis: lack of CC chemokine receptor 5 expression results in a NK1.1+ lymphocyte-associated Th2-type immune response in the intestine. *J. Immunol.* **164**:6303–6312.
- Baird, A. M., R. M. Gerstein, and L. J. Berg. 1999. The role of cytokine receptor signaling in lymphocyte development. *Curr. Opin. Immunol.* **11**: 157–166.
- Bartlett, N. W., K. Buttigieg, S. V. Kotenko, and G. L. Smith. 2005. Murine interferon lambdas (type III interferons) exhibit potent antiviral activity *in vivo* in a poxvirus infection model. *J. Gen. Virol.* **86**:1589–1596.
- Breman, J. G., and D. A. Henderson. 2002. Diagnosis and management of smallpox. *N. Engl. J. Med.* **346**:1300–1308.
- Breman, J. G., and D. A. Henderson. 1998. Poxvirus dilemmas—monkeypox, smallpox, and biologic terrorism. *N. Engl. J. Med.* **339**:556–559.
- Buller, R. M., and G. J. Palumbo. 1991. Poxvirus pathogenesis. *Microbiol. Rev.* **55**:80–122.
- Cao, J. X., P. D. Gershon, and D. N. Black. 1995. Sequence analysis of HindIII Q2 fragment of capripoxvirus reveals a putative gene encoding a G-protein-coupled chemokine receptor homologue. *Virology* **209**:207–212.

9. Carter, G. C., G. Rodger, B. J. Murphy, M. Law, O. Krauss, M. Hollinshead, and G. L. Smith. 2003. Vaccinia virus cores are transported on microtubules. *J. Gen. Virol.* **84**:2443–2458.
10. Chahroudi, A., R. Chavan, N. Kozyr, E. K. Waller, G. Silvestri, and M. B. Feinberg. 2005. Vaccinia virus tropism for primary hematolymphoid cells is determined by restricted expression of a unique virus receptor. *J. Virol.* **79**:10397–10407.
11. Dawson, T. C., M. A. Beck, W. A. Kuziel, F. Henderson, and N. Maeda. 2000. Contrasting effects of CCR5 and CCR2 deficiency in the pulmonary inflammatory response to influenza A virus. *Am. J. Pathol.* **156**:1951–1959.
12. Diven, D. G. 2001. An overview of poxviruses. *J. Am. Acad. Dermatol.* **44**:1–16.
13. Engelmayer, J., M. Larsson, M. Subklewe, A. Chahroudi, W. I. Cox, R. M. Steinman, and N. Bhardwaj. 1999. Vaccinia virus inhibits the maturation of human dendritic cells: a novel mechanism of immune evasion. *J. Immunol.* **163**:6762–6768.
14. Fenner, F. 1989. Risks and benefits of vaccinia vaccine use in the worldwide smallpox eradication campaign. *Res. Virol.* **140**:465–466. (Discussion, **140**:487–491.)
15. Fenner, F., D. A. Henderson, I. Arita, Z. Jezek, and I. D. Ladnyi. 1988. Smallpox and its eradication. World Health Organization, Geneva, Switzerland.
16. Glass, W. G., D. H. McDermott, J. K. Lim, S. Lekhong, S. F. Yu, W. A. Frank, J. Pape, R. C. Cheshier, and P. M. Murphy. 2006. CCR5 deficiency increases risk of symptomatic West Nile virus infection. *J. Exp. Med.* **203**:35–40.
17. Graham, K. A., A. S. Lalani, J. L. Macen, T. L. Ness, M. Barry, L. Y. Liu, A. Lucas, I. Clark-Lewis, R. W. Moyer, and G. McFadden. 1997. The T1/35kDa family of poxvirus-secreted proteins bind chemokines and modulate leukocyte influx into virus-infected tissues. *Virology* **229**:12–24.
18. Harrington, L. E., R. Most Rv, J. L. Whittton, and R. Ahmed. 2002. Recombinant vaccinia virus-induced T-cell immunity: quantitation of the response to the virus vector and the foreign epitope. *J. Virol.* **76**:3329–3337.
19. Hart, C. A., and N. J. Beeching. 2002. A spotlight on anthrax. *Clin. Dermatol.* **20**:365–375.
20. Henderson, D., and B. Moss. 1999. Smallpox and vaccinia. WB Saunders, Philadelphia, PA.
21. Henderson, D. A. 1999. Smallpox: clinical and epidemiologic features. *Emerg. Infect. Dis.* **5**:537–539.
22. Henderson, D. A., T. V. Inglesby, J. G. Bartlett, M. S. Ascher, E. Eitzen, P. B. Jahrling, J. Hauer, M. Layton, J. McDade, M. T. Osterholm, T. O'Toole, G. Parker, T. Perl, P. K. Russell, K. Tonat, et al. 1999. Smallpox as a biological weapon: medical and public health management. *JAMA* **281**:2127–2137.
23. Herold, S., W. von Wulffen, M. Steinmueller, S. Pleschka, W. A. Kuziel, M. Mack, M. Srivastava, W. Seeger, U. A. Maus, and J. Lohmeyer. 2006. Alveolar epithelial cells direct monocyte transepithelial migration upon influenza virus infection: impact of chemokines and adhesion molecules. *J. Immunol.* **177**:1817–1824.
24. Humlova, Z., M. Vokurka, M. Esteban, and Z. Melkova. 2002. Vaccinia virus induces apoptosis of infected macrophages. *J. Gen. Virol.* **83**:2821–2832.
25. Iwasaki, M., T. Mukai, P. Gao, W. R. Park, C. Nakajima, M. Tomura, H. Fujiwara, and T. Hamaoka. 2001. A critical role for IL-12 in CCR5 induction on T cell receptor-triggered mouse CD4(+) and CD8(+) T cells. *Eur. J. Immunol.* **31**:2411–2420.
26. Jacobs, N., R. A. Chen, C. Gubser, P. Najarro, and G. L. Smith. 2006. Intradermal immune response after infection with vaccinia virus. *J. Gen. Virol.* **87**:1157–1161.
27. Johnston, J. B., J. W. Barrett, W. Chang, C. S. Chung, W. Zeng, J. Masters, M. Mann, F. Wang, J. Cao, and G. McFadden. 2003. Role of the serine-threonine kinase PAK-1 in myxoma virus replication. *J. Virol.* **77**:5877–5888.
28. Kunkel, S. L. 1999. Promiscuous chemokine receptors and their redundant ligands play an enigmatic role during HIV-1 infection. *Am. J. Respir. Cell Mol. Biol.* **20**:859–860.
29. Lalani, A. S., J. W. Barrett, and G. McFadden. 2000. Modulating chemokines: more lessons from viruses. *Immunol. Today* **21**:100–106.
30. Lalani, A. S., J. Masters, W. Zeng, J. Barrett, R. Pannu, H. Everett, C. W. Arendt, and G. McFadden. 1999. Use of chemokine receptors by poxviruses. *Science* **286**:1968–1971.
31. Lalani, A. S., T. L. Ness, R. Singh, J. K. Harrison, B. T. Seet, D. J. Kelvin, G. McFadden, and R. W. Moyer. 1998. Functional comparisons among members of the poxvirus T1/35kDa family of soluble CC-chemokine inhibitor glycoproteins. *Virology* **250**:173–184.
32. Locati, M., and P. M. Murphy. 1999. Chemokines and chemokine receptors: biology and clinical relevance in inflammation and AIDS. *Annu. Rev. Med.* **50**:425–440.
33. Mantovani, A. 1999. The chemokine system: redundancy for robust outputs. *Immunol. Today* **20**:254–257.
34. Massung, R. F., V. Jayarama, and R. W. Moyer. 1993. DNA sequence analysis of conserved and unique regions of swinepox virus: identification of genetic elements supporting phenotypic observations including a novel G protein-coupled receptor homologue. *Virology* **197**:511–528.
35. Masters, J., A. A. Hinek, S. Uddin, L. C. Platanius, W. Zeng, G. McFadden, and E. N. Fish. 2001. Poxvirus infection rapidly activates tyrosine kinase signal transduction. *J. Biol. Chem.* **276**:48371–48375.
36. Moss, B. 2001. Poxviridae: the viruses and their replication, vol. 2. Lippincott-Raven Publishers, Philadelphia, PA.
37. Murphy, P. M. 2001. Viral exploitation and subversion of the immune system through chemokine mimicry. *Nat. Immunol.* **2**:116–122.
38. Power, C. A. 2003. Knock out models to dissect chemokine receptor function in vivo. *J. Immunol. Methods* **273**:73–82.
39. Rahbar, R., T. T. Murooka, A. A. Hinek, C. L. Galligan, A. Sassano, C. Yu, K. Srivastava, L. C. Platanius, and E. N. Fish. 2006. Vaccinia virus activation of CCR5 invokes tyrosine phosphorylation signaling events that support virus replication. *J. Virol.* **80**:7245–7259.
40. Rao, A. R., M. Savithri Sukumar, S. Kamalakshi, T. V. Paramasivam, and S. Ramakrishnan. 1972. Further studies with precipitation in gel test in diagnosis of smallpox. I. Studies on detection of antibodies in sera by pig test. *Indian J. Med. Res.* **60**:1254–1260.
41. Reading, P. C., and G. L. Smith. 2003. A kinetic analysis of immune mediators in the lungs of mice infected with vaccinia virus and comparison with intradermal infection. *J. Gen. Virol.* **84**:1973–1983.
42. Reading, P. C., J. A. Symons, and G. L. Smith. 2003. A soluble chemokine-binding protein from vaccinia virus reduces virus virulence and the inflammatory response to infection. *J. Immunol.* **170**:1435–1442.
43. Seet, B. T., and G. McFadden. 2002. Viral chemokine-binding proteins. *J. Leukoc. Biol.* **72**:24–34.
44. Smith, C. A., T. D. Smith, P. J. Smolak, D. Friend, H. Hagen, M. Gerhart, L. Park, D. J. Pickup, D. Torrance, K. Mohler, K. Schooley, and R. G. Goodwin. 1997. Poxvirus genomes encode a secreted, soluble protein that preferentially inhibits beta chemokine activity yet lacks sequence homology to known chemokine receptors. *Virology* **236**:316–327.
45. Suzaki, Y., K. Hamada, T. Nomi, T. Ito, M. Sho, Y. Kai, Y. Nakajima, and H. Kimura. 2008. A small-molecule compound targeting CCR5 and CXCR3 prevents airway hyperresponsiveness and inflammation. *Eur. Respir. J.* **31**:783–789.
46. Turner, G. S. 1967. Respiratory infection of mice with vaccinia virus. *J. Gen. Virol.* **1**:399–402.
47. Wareing, M. D., A. B. Lyon, B. Lu, C. Gerard, and S. R. Sarawar. 2004. Chemokine expression during the development and resolution of a pulmonary leukocyte response to influenza A virus infection in mice. *J. Leukoc. Biol.* **76**:886–895.
48. Williamson, J. D., R. W. Reith, L. J. Jeffrey, J. R. Arrand, and M. Mackett. 1990. Biological characterization of recombinant vaccinia viruses in mice infected by the respiratory route. *J. Gen. Virol.* **71**:2761–2767.
49. Yang, Y. F., T. Mukai, P. Gao, N. Yamaguchi, S. Ono, H. Iwaki, S. Obika, T. Imanishi, T. Tsujimura, T. Hamaoka, and H. Fujiwara. 2002. A non-peptide CCR5 antagonist inhibits collagen-induced arthritis by modulating T cell migration without affecting anti-collagen T cell responses. *Eur. J. Immunol.* **32**:2124–2132.
50. Yu, Q., Jones, B., Hu, N., Chang, H., Ahmad, S., Liu, J., Parrington, M., and M. Ostrowski. 2006. Comparative analysis of tropism between canarypox (ALVAC) and vaccinia viruses reveals a more restricted and preferential tropism of ALVAC for human cells of the monocytic lineage. *Vaccine* **24**:6376–6391.